



Contents lists available at ScienceDirect

Chinese Chemical Letters

journal homepage: www.elsevier.com/locate/ccl

Communication

Selective adsorption behaviors of guest molecules COR in the hexamer host networks at liquid/solid interface



Xiaokang Li^{a,b}, Jianqiao Li^{a,b}, Chunyu Ma^{a,b}, Chen Chen^{a,b}, Siqi Zhang^{a,b}, Bin Tu^{a,*},
Wubiao Duan^{b,**}, Qingdao Zeng^{a,c,*}

^a CAS Key Laboratory of Standardization and Measurement for Nanotechnology, CAS Center for Excellence in Nanoscience, National Center for Nanoscience and Technology (NCNST), Beijing 100190, China

^b Department of Chemistry, School of Science, Beijing Jiaotong University, Beijing 100044, China

^c Center of Materials Science and Optoelectronics Engineering, University of Chinese Academy of Sciences, Beijing 100049, China

ARTICLE INFO

Article history:

Received 1 June 2020

Received in revised form 22 July 2020

Accepted 27 July 2020

Available online 29 July 2020

Keywords:

Scanning probe microscopy (STM)

Selective adsorption

Host-guest chemistry

Supramolecular chemistry

Aromatic carboxylic acid

ABSTRACT

Here, the selective adsorption behaviors of guest molecule COR in two hexamer host grids were investigated by means of scanning tunnelling microscope (STM). The assembled structures of small functional organic molecules TTBA and TATBA were thermodynamically stable. Interestingly, the introduction of the guest molecule COR destroyed the original hexamer structure of TTBA and combined with it to form a new triangular host-guest system. Different from TTBA, the introduction of the guest molecule COR did not affect the six-membered ring structure of TATBA. Furthermore, the co-assembly structure of TTBA/TATBA/COR was established and the guest molecule COR showed preferential adsorption to the TATBA host grid. Density functional theory (DFT) calculations had been performed to disclose the mechanism of the involved assemblies.

© 2020 Chinese Chemical Society and Institute of Materia Medica, Chinese Academy of Medical Sciences. Published by Elsevier B.V. All rights reserved.

The host-guest chemistry of the surface/interface has attracted much attention due to its broad prospects in nanotechnology and nanomaterials [1–4]. The main reason for this is that the host-guest chemistry provides an interesting strategy for the construction of ordered specific structures at the molecular level [5]. It is well known that host-guest chemistry is a branch of supramolecular chemistry, which constructs functional complexes through non-covalent interactions among molecules [6–12]. In general, in order to obtain well ordered specific complexes, the rigid host networks can be used to accommodate the guest molecules. The guest molecules filled in the cavity of the rigid host networks cannot change the original structures of the host templates [13–15]. However, the host networks constructed by small functional organic molecules [16–20] can respond to the guest molecules flexibly through the breakage and generation of noncovalent bonds, which is more conducive to enhance the stability of the structure. Another significant point is that conjugated systems of

aromatic rings are helpful to facilitate electron transport, thus the self-assembled structures are more prone to have special optical, electrical, and magnetic properties. Scanning tunneling microscope (STM), with atomic-level resolution, is an essential characterization tool for studying host-guest systems [6,21–24]. With the help of STM, the assembly structures and dynamic behaviors of the host-guest systems can be observed and studied directly under atmospheric conditions [25–31].

Up to now, there have been many researches on host-guest systems, including the fabrication of controllable nanoparticles in the host networks [32], efficient photochemical reactions [33] and preferential adsorption of different guests on different host networks [34]. However, studies on the dynamic selective adsorption behavior of a single type of guest molecule in multiple host networks are rare. Peng *et al.* studied the adsorption behavior of the same guest in host templates based on different driving forces [20]. Li *et al.* reported the non-selective adsorption of guest molecule COR in two flower-like structures formed by two kinds of C₃-symmetric hexacarboxylic acid molecules [35–39].

Here, the preferential adsorption behavior of the same guest in different host networks would be further investigated. Two kinds of small functional organic molecules with three carboxyl groups, benzo[1,2-b:3,4-b':5,6-b'']tristhiophene-2,5,8-tricarboxylic acid (TTBA) and 4,4',4''-(1,3,5-triazine-2,4,6-triyl)tribenzoic acid

* Corresponding authors at: CAS Key Laboratory of Standardization and Measurement for Nanotechnology, CAS Center for Excellence in Nanoscience, National Center for Nanoscience and Technology (NCNST), Beijing 100190, China.

** Corresponding author.

E-mail addresses: tub@nanocr.cn (B. Tu), wbd@bjtu.edu.cn (W. Duan), zengqd@nanocr.cn (Q. Zeng).

(TATBA), are chosen to construct host networks. With the help of STM, the co-assembly behavior of the guest molecule coronene (COR) in the host networks formed by TTBTA and TATBA are studied separately. The solid substrate used in the experiment is highly oriented pyrolytic graphite (HOPG). Combined with density functional theory (DFT) calculations, the mechanism of selective adsorption of the guest molecule COR in the host networks TTBTA and TATBA was further studied. The chemical structures of TTBTA, TATBA and COR are shown in Scheme 1.

In this research, TTBTA and TATBA molecules were purchased from Jilin Chinese Academy of Sciences-Yanshen Technology Co., Ltd. COR and 1-heptanoic acid (HA) were purchased from J&K Scientific. All molecules including the host molecules (TTBTA, TATBA) and the guest molecule (COR) were dissolved in the heptanoic acid respectively with the solution concentrations not exceeding 10^{-4} mol/L. The assemblies were prepared by subsequent deposition of the components onto a freshly cleaned HOPG (grade ZYB, NTMDT, Russia) surface. TTBTA or TATBA solution was deposited on HOPG, and then detected by STM. Afterwards, COR dissolved in 1-heptanoic acid was added to the monocomponent system of TTBTA and TATBA followed by STM detection. All experiments were performed at room temperature.

The STM measurements were performed by means of a Nanoscope IIIa scanning probe microscope (Bruker, USA) in constant current mode under ambient conditions. As the STM tips, it is prepared by mechanically cutting the Pt/Ir wire (80/20).

In this work, theoretical analysis of STM data was carried out with the DMol³ mode [40]. We applied DFT-D3 method (Perdew-Burke-Ernzerhof correlation energy PBE [41] as the DFT functional applied in the generalized gradient approximation (GGA) to describe exchange and correlation), in which the atom-pair wise (atom-triple wise) dispersion correction can be added to the standard Kohn–Sham density functional theory (KS-DFT) energies (and gradient) [42]:

$$E_{\text{DFT-D3}} = E_{\text{KS-DFT}} + E_{\text{disp}} \quad (1)$$

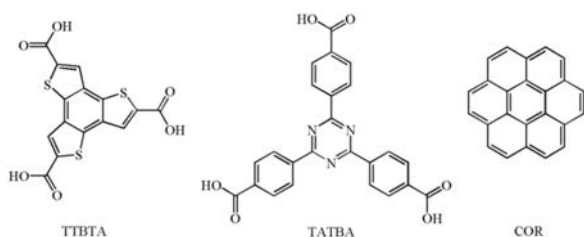
with E_{disp} being the sum of the two- and three-body contributions to the dispersion energy:

$$E_{\text{disp}} = E_{(2)} + E_{(3)} \quad (2)$$

The most important two-body term is given at long range by

$$E_{\text{disp}} = \frac{1}{2} \sum_{A \neq B} \sum_{n=6,8} S_n \frac{C_n^{AB}}{r_{AB}^n} \quad (3)$$

here, C_n^{AB} denotes the averaged (isotropic) n th-order dispersion coefficient for atom pair AB, and r_{AB}^n is their internuclear distance. S_n is a functional-dependent scaling factor. We introduced numerical basis sets into the large system and calculated all-electron ones which were on the medium grid. In the self-consistent field procedure, the convergence standard of the energy and electron density was chosen as 10^{-5} a.u. In addition, initial models were supposed to be consistent with experimental parameters and all structures were optimized further. When the



Scheme 1. Chemical structures of TTBTA, TATBA and guest molecule COR investigated in this paper.

energy and density convergence criterion are reached, we could obtain the optimized parameters and the interaction energy between adsorbates.

Considering that the interaction between adsorbates and substrate is mainly van der Waals interaction, the dispersion corrections (for example, the Grimme's dispersion corrections) should be included in the results. We have performed DFT-D method to estimate the interaction energy of the adsorbate with graphene. The DFT-D method really can be considered successfully now on thousands of different systems including inter- and intramolecular cases ranging from rare gas dimers to huge graphene sheets [36]. The graphene layer was referred to as a periodic arrangement of orthorhombic unit cells including two carbon atoms, wherein the distance in the normal direction in the superlattice was 40 Å. When modeling the adsorbates on graphene, we used graphene supercells and sampled the Brillouin zone by a $1 \times 1 \times 1$ k-point mesh. The interaction energy E_{inter} of adsorbates with graphite is given by $E_{\text{inter}} = E_{\text{tot}}(\text{adsorbates/graphene}) - E_{\text{tot}}(\text{isolated adsorbates in vacuum}) - E_{\text{tot}}(\text{graphene})$.

After depositing a droplet of TTBTA solution on HOPG, the large-scale self-assembly structures were detected at the interface of heptanoic acid/HOPG, and was shown in Fig. S1a (Supporting information). It is worth noting that two types of structures can be observed, one is a loose structure formed by two carboxyl groups head to head, and the other is a close-packed network formed side by side. The first kind of structure has been studied to host C₆₀ molecule [43], so here we focus on the second kind of close-packed network. As shown in Fig. 1a, an ordered hexamer grid can be clearly observed. The bright spots of the approximate triangle correspond to TTBTA molecules, which were aligned edge-to-edge. The central cavity of the hexamer structure is formed by the carboxyl groups of six TTBTA molecules in a fenced manner. The molecular model of TTBTA structures (Fig. 1b) indicated that a circular cavity with an inner diameter of 0.8 ± 0.1 nm was composed of carboxyl groups connected by hydrogen bonds. Moreover, each carboxyl group of the TTBTA molecule simultaneously formed two hydrogen bonds with the two carboxyl groups

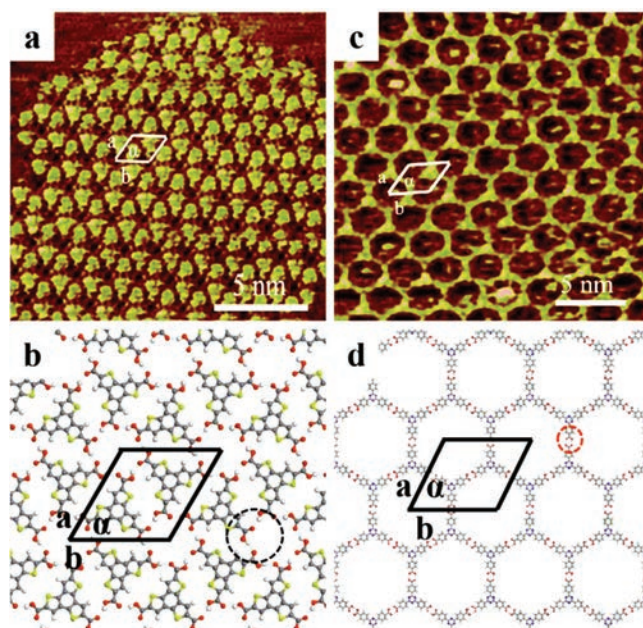


Fig. 1. (a) High-resolution STM image of TTBTA structures at the HA/HOPG interface ($I_{\text{set}} = 375.4$ pA, $V_{\text{bias}} = 601.8$ mV). (b) Proposed molecular model of TTBTA hexamer grid structures. (c) High-resolution STM image of TATBA structures at the HA/HOPG interface ($I_{\text{set}} = 363.2$ pA, $V_{\text{bias}} = 582.0$ mV). (d) Proposed molecular model of TATBA six-membered ring structures.

Table 1

The experimental (exptl.) and calculated (calcd.) unit cell parameters for the templates and host-guest architectures.

Samples		a (nm)	b (nm)	α (degree)
TTBTA	exptl.	1.7 ± 0.1	1.7 ± 0.1	60 ± 2
	calcd.	1.70	1.66	60.0
TTBTA/COR	exptl.	1.8 ± 0.1	1.8 ± 0.1	49 ± 2
	calcd.	1.80	1.80	48.0
TATBA	exptl.	3.1 ± 0.1	3.1 ± 0.1	60 ± 2
	calcd.	3.14	3.14	60.0
TATBA/COR	exptl.	3.1 ± 0.1	3.1 ± 0.1	59 ± 2
	calcd.	3.14	3.14	60.0

of two adjacent TTBTA molecules (as shown by the black circle in Fig. 1b). A unit cell of the molecular model was marked in Fig. 1a, $a = b = 1.7 \pm 0.1$ nm and $\alpha = 60 \pm 2^\circ$ (Table 1). The hexameric structure of TTBTA allowed the three carboxyl groups of each molecule to combine with the carboxyl groups of adjacent molecules to form three pairs of hydrogen bonds, ensuring the saturation of the hydrogen bonds of the carboxyl groups.

The highly ordered arrangement of the TATBA structure over a wide range can be observed, as shown in Fig. S1b (Supporting information). Similar to TTBTA molecule, as shown in high-resolution Fig. 1c, the bright point of the triangle corresponded to the TABAA molecule, but it can be clearly seen that the triangle shape corresponding to TATBA is more regular and obvious. The TATBA molecules could self-assemble into regular six-membered rings, and the inner diameter of the central cavity is 2.2 ± 0.1 nm. The reason for this is that the angle between the two carboxyl groups in the molecule is 120° , and it takes six pairs of carboxyl groups to form a closed loop geometrically. In addition, the 1,3,5-triazine cores of the TATBA molecules were used as the vertex of the hexagon, and two carboxyl groups at the end of two TATBA molecules interact in a head-to-head manner to form a pair of hydrogen bonds (as shown by the red circle in Fig. 1d). The parameters of the unit cell, measured from Fig. 1c, were $a = b = 3.1 \pm 0.1$ nm, $\alpha = 60^\circ \pm 2^\circ$ (Table 1). In these two hexamer structures, the three carboxyl groups of TTBTA and TATBA all participated in self-assembly to form hydrogen bonds, releasing more energy, which makes the energy of the intermolecular system lower and more stable. Both TTBTA and TATBA cavities can accommodate guest molecules, so the study of the selective behavior of guest molecules on these two molecular templates has attracted our interest.

When the COR solution was added to the mono-component system of TTBTA, a large-scale STM image of the TTBTA/COR co-assembled structures was shown in Fig. S2a (Supporting information). Interestingly, after the introduction of the guest molecule COR, the original hexamer structure of TTBTA was destroyed and combined with it to form a new triangular host-guest system. In the high-resolution STM image (Fig. 2a), it is shown that the COR molecules (shown as blue circles in Fig. 2a) represented by circular bright spots are located in a triangular cavity formed by three TTBTA molecules (shown as white circles in Fig. 2a). This transformation of the TTBTA molecule host network was advantageous for the immobilization of guest molecules COR in the cavity (Fig. 2b). The unit cell parameters were measured $a = b = 1.8 \pm 0.1$ nm and $\alpha = 48^\circ \pm 2^\circ$ (Table 1). With the introduction of COR, the interactions between molecules and substrate in the architecture were much strengthened and resulted in the reduction of the total energy per unit area (-0.485 kcal mol $^{-1}$ Å $^{-2}$), which was helpful for the stable existence of TTBTA/COR co-assembled structures on HOPG. The DFT results (Table 2) revealed that the total energies per unit areas of TTBTA/COR co-assembled structures (-0.485 kcal mol $^{-1}$ Å $^{-2}$) was lower than that of TTBTA's pure architecture (-0.398 kcal mol $^{-1}$ Å $^{-2}$), so the host-guest

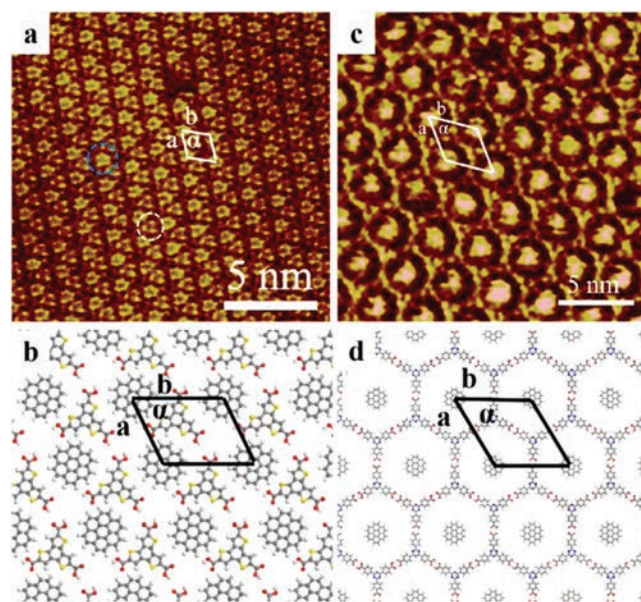


Fig. 2. (a) High-resolution STM image of TTBTA/COR structures at the HA/HOPG interface ($I_{\text{set}} = 152.6$ pA, $V_{\text{bias}} = 919.8$ mV). (b) Proposed molecular model of TTBTA/COR. (c) High-resolution STM image of TATBA/COR structures at the HA/HOPG interface ($I_{\text{set}} = 183.1$ pA, $V_{\text{bias}} = 911.9$ mV). (d) Proposed molecular model of TATBA/COR.

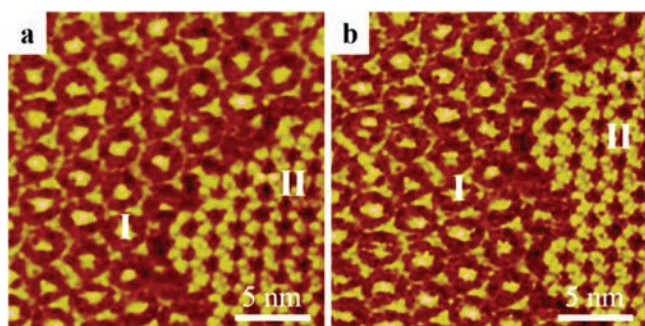
architectures could be constructed after the addition of COR. Furthermore, when COR molecules were deposited on the TATBA templates, a large-scale STM image of the TATBA/COR co-assembled architectures was shown in Fig. S2b (Supporting information). Different from TTBTA, the introduction of the guest molecule COR did not affect the six-membered ring structures of TATBA (Fig. 2c). The high-resolution image indicated that a guest molecule COR was immobilized in the center of the cavity of the six-membered ring. The parameters of the unit cell, measured from Fig. 2d, were $a = b = 3.1 \pm 0.1$ nm, $\alpha = 60^\circ \pm 2^\circ$. Similar to TTBTA, due to the introduction of COR, the total energy per unit area of TATBA/COR co-assembled structure (-0.402 kcal mol $^{-1}$ Å $^{-2}$) was lower than that of TATBA's pure architecture (-0.282 kcal mol $^{-1}$ Å $^{-2}$), which is also conducive to the construction of TATBA/COR co-assembled structure and its stable existence on HOPG.

To further investigate the selective adsorption of COR in the two templates, the three-component structure of the TTBTA/TATBA/COR system was built. As shown in the high-resolution image (Figs. 3a and b), when the two host networks formed by TTBTA and TATBA coexist, the guest molecule COR would be selectively adsorbed in the cavities formed by TATBA (region I), while the hexamer grid formed by TTBTA would not be affected (region II). Although the DFT results showed that the total energy per unit area of TTBTA/COR system (-0.485 kcal mol $^{-1}$ Å $^{-2}$) was lower than that of TATBA/COR (-0.402 kcal mol $^{-1}$ Å $^{-2}$), this selective assembly was probably due to the steric hindrance effect that played an important role in the dynamic process of COR's preferential adsorption of the two host networks. We observed that the cavities formed by TTBTA were smaller than those formed by TATBA, into which a COR molecule cannot enter (The measured diameters of cavities formed by TTBTA and TATBA were about 0.7 ± 0.1 and 2.2 ± 0.1 nm, respectively, and the size of single COR molecule was about 1.0 nm). During the process of COR enter the cavities formed by TTBTA, the original host structure must be broken first, and then reassembled. On the other hand, COR can directly enter into the host structure of TATBA without obstacles. Therefore, COR molecules may be preferentially adsorbed in the host network

Table 2

Total energies and energies per unit area for the assembly structures of TTBTA, TTBTA/COR, TATBA and TATBA/COR.

Sample	Interactions between molecules (kcal/mol)	Interactions between molecules and substrate (kcal/mol)	Total energy (kcal/mol)	Total energy per unit area (kcal mol ⁻¹ Å ⁻²)
TTBTA	-62.761	-51.211	-113.972	-0.398
TTBTA/COR	-10.218	-106.144	-116.362	-0.485
TATBA	-126.256	-112.351	-238.607	-0.282
TATBA/COR	-128.231	-181.251	-309.482	-0.402

**Fig. 3.** (a,b) High-resolution STM image of TTBTA/TATBA/COR co-assembly structures at the HA/HOPG interface ($I_{\text{set}} = 183.1$ pA, $V_{\text{bias}} = 911.9$ mV).

of TATBA instead of TTBTA, forming the thermodynamic stable TATBA/COR architecture.

In summary, the assembly behavior of two small functional organic molecules, TTBTA and TATBA, was studied by STM and DFT calculations. Both TTBTA and TATBA molecules can self-assemble into six-membered ring structure through hydrogen bonding interactions, but two kinds of cavities with different sizes were formed due to the different binding directions of hydrogen bonds between carboxyl groups. The self-assembled networks of TTBTA and TATBA could be used as molecular templates to accommodate the guest molecule COR. Interestingly, the introduction of the guest molecule COR destroyed the original hexamer structure of TTBTA and combined with it to form a new triangular host-guest system. Different from TTBTA, the introduction of the guest molecule COR did not affect the six-membered ring structure of TATBA. Furthermore, the co-assembly structure of TTBTA/TATBA/COR was established. The guest molecule COR showed preferential adsorption to the TATBA host grid, and it was explained and analyzed by the combination of DFT calculations and steric hindrance effect. This research provided a deep insight of the selective adsorption behavior of a single guest in multiple host templates.

Declaration of competing interest

The authors declare that they have no known competing financial interests or personal relationships that could have appeared to influence the work reported in this paper.

Acknowledgments

This work was supported by the National Basic Research Program of China (No. 2016YFA0200700), the National Natural Science Foundation of China (Nos. 21773041 and 21972031) and the Strategic Priority Research Program of Chinese Academy of Sciences (No. XDB36000000).

Appendix A. Supplementary data

Supplementary material related to this article can be found, in the online version, at doi:<https://doi.org/10.1016/j.ccl.2020.07.049>.

References

- [1] J. Xu, W.X. Liu, Y.F. Geng, et al., *Nanoscale* 9 (2017) 2579–2584.
- [2] M. O. Blunt, J.C. Russell, M.D. Gimenez-Lopez, et al., *Nat. Chem.* 3 (2011) 74–78.
- [3] K. Iritani, K. Tahara, S. De Feyter, Y. Tobe, *Langmuir* 33 (2017) 4601–4618.
- [4] S.Y. Li, T. Chen, J.Y. Yue, D. Wang, L.J. Wan, *Chem. Commun.* 53 (2017) 11095–11098.
- [5] S. Stepanow, M. Lingenfelder, A. Dmitriev, et al., *Nat. Mater.* 3 (2004) 229–233.
- [6] J. Adisojoso, K. Tahara, S. Okuhata, et al., *Angew. Chem. Int. Ed.* 48 (2009) 7353–7357.
- [7] L.X. Cheng, X. Peng, S.Q. Zhang, et al., *Appl. Surf. Sci.* 31 (2018) 1036–1043.
- [8] J. Plas, O. Ivashenko, N. Martsinovich, M. Lackinger, S. De Feyter, *Chem. Commun.* 52 (2016) 68–71.
- [9] Y.F. Geng, S. Wang, M.Q. Shen, et al., *ACS Omega* 2 (2017) 5611–5617.
- [10] X.K. Li, S.Q. Zhang, J.Q. Li, et al., *New J. Chem.* 43 (2019) 13315–13325.
- [11] S. Lee, B.E. Hirsch, Y. Liu, et al., *Chem. Eur. J.* 22 (2016) 560–569.
- [12] J.D. Xue, K. Deng, B. Liu, et al., *RSC Adv.* 5 (2015) 39291–39294.
- [13] Y. Kikkawa, H. Kihara, M. Takahashi, et al., *J. Phys. Chem. B* 114 (2010) 16718–16722.
- [14] S.J.H. Griessl, M. Lackinger, F. Jamitzky, et al., *J. Phys. Chem. B* 108 (2004) 11556–11560.
- [15] D.X. Wu, K. Deng, Q.D. Zeng, C. Wang, *J. Phys. Chem. B* 109 (2005) 22296–22300.
- [16] E. Ghijsens, H. Cao, A. Noguchi, et al., *Chem. Commun.* 51 (2015) 4766–4769.
- [17] S.B. Lei, K. Tahara, X.L. Feng, et al., *J. Am. Chem. Soc.* 130 (2008) 7119–7129.
- [18] K. Gruber, C. Rohr, L.J. Scherer, et al., *Adv. Mater.* 23 (2011) 2195–2198.
- [19] J.M. MacLeod, O. Ivashenko, C.Y. Fu, et al., *J. Am. Chem. Soc.* 131 (2009) 16844–16850.
- [20] X. Peng, Y.F. Geng, M. Zhang, et al., *Nano Res.* 12 (2019) 537–542.
- [21] X. Zhang, T. Chen, H.J. Yan, et al., *ACS Nano* 4 (2010) 5685–5692.
- [22] X.R. Miao, L. Xu, Y.J. Li, et al., *Chem. Commun.* 46 (2010) 8830–8832.
- [23] J.T. Wu, J.X. Li, M.Q. Dong, et al., *J. Phys. Chem. C* 122 (2018) 22597–22604.
- [24] S. De Feyter, F.C. De Schryver, *Chem. Soc. Rev.* 32 (2003) 139–150.
- [25] J. Lu, S.B. Lei, Q.D. Zeng, et al., *J. Phys. Chem. B* 108 (2004) 5161–5165.
- [26] X. Zhang, S.S. Li, H. Lin, et al., *J. Electroanal. Chem.* 656 (2011) 304–311.
- [27] H. Dai, W. Yi, K. Deng, H. Wang, Q.D. Zeng, *ACS Appl. Mater. Interfaces* 8 (2016) 21095–21100.
- [28] K. Tahara, K. Nakatani, K. Iritani, S. De Feyter, Y. Tobe, *ACS Nano* 10 (2016) 2113–2120.
- [29] S.Q. Zhang, J. Zhang, K. Deng, et al., *Phys. Chem. Chem. Phys.* 17 (2015) 24462–24467.
- [30] M. Shen, Z. Luo, S.Q. Zhang, et al., *Nanoscale* 8 (2016) 11962–11968.
- [31] W. Huang, T.Y. Zhao, M.W. Wen, et al., *J. Phys. Chem. C* 118 (2014) 6767–6772.
- [32] Y.F. Geng, M.Q. Liu, J.D. Xue, et al., *Chem. Commun.* 51 (2015) 6820–6823.
- [33] J.D. Xue, J. Xu, F.Y. Hu, et al., *Phys. Chem. Chem. Phys.* 16 (2014) 25765–25769.
- [34] Y.T. Shen, K. Deng, X.M. Zhang, et al., *J. Phys. Chem. C* 115 (2011) 19696–19701.
- [35] J.Q. Li, B. Tu, X.K. Li, et al., *Chem. Commun.* 55 (2019) 11599–11602.
- [36] J.Q. Li, X.Y. Zu, Y.X. Qian, et al., *Chin. Chem. Lett.* 31 (2020) 10–18.
- [37] J.F. Hou, B. Tu, Q.D. Zeng, C.L. Zhan, J.N. Yao, *Chin. Chem. Lett.* 31 (2020) 353–356.
- [38] J. Xu, Y.B. Li, L.J. Wang, et al., *Chin. Chem. Lett.* 30 (2019) 767–770.
- [39] J.Q. Li, Y.X. Qian, W.B. Duan, Q.D. Zeng, *Chin. Chem. Lett.* 30 (2019) 292–298.
- [40] B.J. Delley, *J. Chem. Phys.* 113 (2000) 7756–7764.
- [41] J.P. Perdew, K. Burke, M. Ernzerhof, *Phys. Rev. Lett.* 77 (1996) 3865–3868.
- [42] S. Grimme, J. Antony, S. Ehrlich, H. Krieg, *J. Chem. Phys.* 132 (2010) 154104.
- [43] J.M. MacLeod, O. Ivashenko, C. Fu, et al., *J. Am. Chem. Soc.* 131 (2009) 16844–16850.